

AN EXTREME [O III] EMITTER AT $z = 3.2$: A LOW METALLICITY LYMAN CONTINUUM SOURCE

S. de Barros¹ and E. Vanzella¹

Abstract. We investigate the physical properties of a Lyman continuum emitter candidate at $z = 3.212$ with photometric coverage from U to MIPS $24\mu\text{m}$ band and VIMOS/VLT and MOSFIRE/Keck spectroscopy. Investigation of the UV spectrum confirms a direct spectroscopic detection of the Lyman continuum emission with $S/N > 5$. Non-zero $\text{Ly}\alpha$ flux at the systemic redshift and high Lyman- α escape fraction suggest a low H I column density. The weak C and Si low-ionization absorption lines are also consistent with a low covering fraction along the line of sight. The [O III] $\lambda\lambda 4959, 5007 + \text{H}\beta$ equivalent width is one of the largest reported for a galaxy at $z > 3$ ($\text{EW}([\text{O III}]\lambda\lambda 4959, 5007 + \text{H}\beta) \simeq 1600\text{\AA}$, rest-frame; 6700\AA observed-frame) and the NIR spectrum shows that this is mainly due to an extremely strong [OIII] emission. The large observed [O III]/[O II] ratio (> 10) and high ionization parameter are consistent with prediction from photoionization models in case of a density-bounded nebula scenario. This source is currently the first high- z example of a Lyman continuum emitter exhibiting indirect and direct evidences of a Lyman continuum leakage and having physical properties consistent with theoretical expectation from Lyman continuum emission from a density-bounded nebula.

Keywords: Galaxies: high-redshift; Galaxies: evolution; Galaxies: ISM; Galaxies: starburst

1 Introduction

A number of surveys at $1 < z < 3.5$ both from the ground and with the Hubble Space Telescope (*HST*), have looked for ionizing photons by means of imaging or spectroscopy and there have been some claims of detections (Steidel et al. 2001; Shapley et al. 2006; Nestor et al. 2013; Mostardi et al. 2013, 2015). However several other surveys reported only upper limits (Siana et al. 2010; Bridge et al. 2010; Malkan et al. 2003; Vanzella et al. 2010, 2012; Boutsia et al. 2011; Grazian et al. 2015). Attempts at identifying individual galaxies at $z > 1$ with Lyman continuum (LyC , $< 912\text{\AA}$) emission have so far been unsuccessful and have provided upper limits on the $f_{\text{esc}}(\text{LyC})$ of the order of few percent ($< 5\%$; Vanzella et al. 2012; Siana et al. 2015). This could be due to the rarity of relatively bright ionizing sources, as a consequence of the combination of view-angle effects (Cen & Kimm 2015), stochastic intergalactic opacity (Inoue & Iwata 2008; Inoue et al. 2014) and possibly intrinsically low escaping ionizing radiation on average, in the luminosity regime explored so far ($L > 0.1L^*$, e.g., Vanzella et al. 2010).

We have identified two Lyman continuum leakers in Vanzella et al. (2015), hereafter V15: *Ion1* and *Ion2*. These galaxies have been selected as Lyman continuum emitters through a photometric selection which is based on the comparison between the observed photometric fluxes and colors probing the Lyman continuum emission and predictions from the combination of spectral synthesis models (e.g., Bruzual & Charlot 2003) and intergalactic medium (IGM) transmissions (Inoue et al. 2014).

In this work we present the source with one of the largest [O III] $\lambda\lambda 4959, 5007$ line equivalent width currently known ($\text{EW} \sim 1500\text{\AA}$, rest-frame) at $z > 3$ and with a plausible leakage of ionizing radiation. Ultraviolet (VLT/VIMOS), optical and NIR (Keck/MOSFIRE) rest-frame spectroscopy are presented, as well as a detailed multi-frequency analysis with the aim to test possible signatures of linking Lyman continuum.

¹ INAF–Osservatorio Astronomico di Bologna, via Ranzani 1, I-40127 Bologna, Italy, email: stephane.debarros@oabo.inaf.it

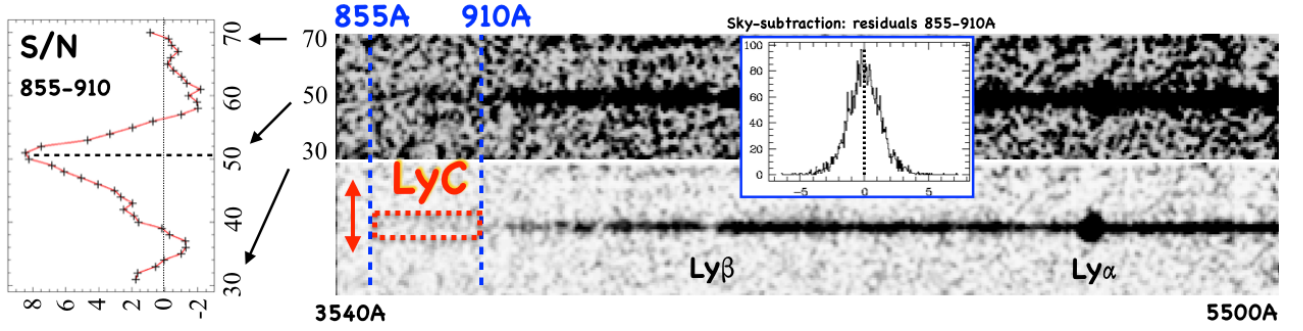


Fig. 1. Two-dimensional LR VIMOS UV spectrum of *Ion2*. We show the moving average calculated within a rectangular aperture ($855\text{-}910\text{\AA} \times 1.25''$, red-dotted rectangle) in the spatial direction divided by its r.m.s. on the left side. A signal is detected at $\lambda < 912\text{\AA}$ with $S/N > 5$. The inset shows the pixel distribution of the background after sky-subtraction in the region $855\text{-}910\text{\AA}$ (derived from the S/N spectrum). No significant systematic effects are present.

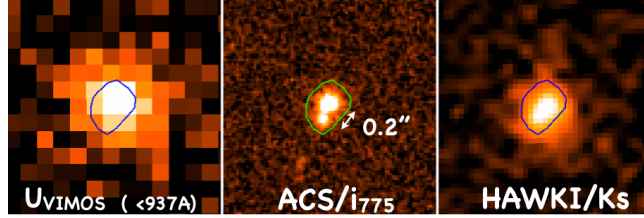


Fig. 2. Ground based VLT/VIMOS U-band observation of *Ion2* at a resolution of $0.2''/\text{pixel}$ (left panel). The contour of the system (derived from the ACS/ i_{775} band, center panel) is indicated and superimposed in blue to the VIMOS U-image and to the HAWK-I K_s image (right panel). The cutouts are $2.6''$ vs. $2.6''$.

2 Spectroscopic detection and spatial distribution of the Lyman continuum emission

The VIMOS LR spectrum of *Ion2* shows a clear signal detected blueward the Lyman limit. We performed a careful reanalysis of the *Ion2* low-resolution UV spectrum by computing the moving average of the flux at $\lambda < 910\text{\AA}$ and we find a signal with $S/N > 5$ (Figure 1). While several systematics can affect the derivation of the LyC signal (e.g., background subtraction, Shapley et al. 2006), we use different methods of sky subtraction (ABBA method and polynomial fitting with different orders) and they all provide consistent results. In particular the same moving average in the LyC region calculated over the S/N two-dimensional spectrum we derived with ABBA method (see Vanzella et al. 2014) produces stable results with no significant systematics and a signal ($> 5\sigma$) at the same spatial position of the target. This signal can be interpreted as a direct detection of the Lyman continuum emission, but the presence of the two components in the *HST* images can cast some doubts about the origin of this detection. However, assuming that the faintest component keeps the same magnitude as the derived B_{435} magnitude (27.25 ± 0.24 ; V15) at shorter wavelengths, the average S/N in the range $3600\text{-}3840\text{\AA}$ is ~ 0.5 per pixel (from ETC). Averaging over 20 pixels, as we did in Figure 1, we would expect $S/N \sim 2.2$. In addition, the B -band dropout signature of such a component ($B - V = 0.62$, V15) between the B_{435} and V_{606} prevents a possible increased emission approaching the U -band, unless an emission feature is boosting the U -band magnitude. In such a case the only possible line would be $[\text{O II}]\lambda 3727$ which would also imply a certain amount of star-formation activity, that in turns would be detectable through Balmer and/or Oxygen lines in the wide spectral range probed here. The most likely explanation is that the spectroscopic detection is due to a Lyman continuum emission emerging from the brightest *Ion2* component. Furthermore, the ground-based VLT/VIMOS U -band spatial distribution shows that most of the U -band flux is emitted from the brightest component (Figure 2).

However, the U -band probes both ionizing *and* non-ionizing photons ($\lambda < 937\text{\AA}$), so a fraction of the signal is not due only to Lyman continuum photons, and the ground-based observations are clearly limited in terms of resolution, as seen in Figure 2.

The only way to clarify the exact position and the detailed spatial distribution of the Lyman continuum emission is to perform dedicated *HST* observations. A proposal to observe *Ion2* with *HST*/F336W (17 orbits)

has been recently approved (PI: Vanzella, cycle 23). Hopefully, emission line diagnostics can be used to characterize the gaseous and stellar content of *Ion2* and provide some hints about a Lyman continuum leakage, as discussed in the next Section.

3 Lyman continuum leakage signatures

We use VLT/VIMOS and Keck/MOSFIRE spectroscopy to obtain a wide *Ion2* spectral coverage with $850\text{\AA} < \lambda < 5700\text{\AA}$ (rest-frame).

The first property derived from emission lines is the spectroscopic redshift. As already reported in V15, the C III] $\lambda 1906.68 - 1908.68$ transition is clearly detected in the VIMOS MR spectrum (with $S/N = 8$). This feature shows a symmetric shape with a relatively large FWHM ($= 400\text{ km s}^{-1}$) with respect to other lines like Ly α and [O III], suggesting the two components have similar intensities, even if they are blended and non resolved. The redshift we derive from C III] is fully consistent with the redshift of Oxygen lines $4959 - 5007\text{\AA}$ identified in the MOSFIRE spectrum. This provides a robust estimate of the systemic redshift, $z = 3.2127 \pm 0.0008$.

We derive ionization parameter, Oxygen and Carbon abundances using a modified version of the HII-CHI-mistry code (Pérez-Montero 2014), adapted to provide metallicity, C/O and ionization parameter in a Te-consistent framework, based on the comparison of the observed UV and optical nebular lines with a grid of CLOUDY photoionization models (Ferland et al. 2013). The derived abundances and ionization parameter are $12 + \log(\text{O}/\text{H}) = 8.07 \pm 0.44$, $\log(\text{C}/\text{O}) = -0.80 \pm 0.13$, and $\log U = -2.25 \pm 0.81$. Both set of lines lead to low metallicity and high ionization parameter (in the following, we consider the results obtain with all the line measurements and upper limits). *Ion2* metallicity is similar to the typical green pea metallicity ($12 + \log(\text{O}/\text{H}) = 8.05 \pm 0.14$, Amorín et al. 2010). The metallicity and ionization parameter are also consistent with extreme emission-line galaxies up to $z \sim 3.5$ (Amorín et al. 2014b,a, 2015). The metallicity of *Ion2* is also consistent with the mean metallicity of star-forming galaxies selected through their extreme EW([O III]) (Maseda et al. 2014; Amorín et al. 2015; Ly et al. 2014).

We compare the metallicity and the ionization parameter with the results presented in Nakajima & Ouchi (2014). Overall, *Ion2* has a lower metallicity than all other galaxy populations presented in their work and one of the highest ionization parameter. The higher ionization parameter is in line with a possible Lyman continuum leaking that could be explained with a low neutral hydrogen column density. Also, the *Ion2* extreme [O III] $\lambda 5007$ /[O II] ratio, the metallicity, and the ionization parameter are consistent with CLOUDY models with a non zero Lyman continuum escape fraction (Nakajima & Ouchi 2014, , Figure 11).

The identification of Lyman continuum leakage from Green pea galaxies is a current line of research (e.g., Jaskot & Oey 2014; Nakajima & Ouchi 2014; Borthakur et al. 2014; Yang et al. 2015) and the Green pea nature of *Ion2* and its LyC leakage represent the first concrete attempt to link these two properties. *Ion2* represents an extreme case of Green pea galaxy, being the highest redshift ($z > 3$) ultra-strong Oxygen emitter (with $\text{EW}([\text{O III}]\lambda\lambda 4959, 5007) \sim 1100\text{\AA}$) currently known. The Lyman continuum leakage observed in *Ion2* allow us to investigate the relationship between the LyC leakage and physical and morphological properties. However, as shown in Stasińska et al. (2015), the [O III]/[O II] ratio is also related to the specific star formation rate and the metallicity: the [O III]/[O II] ratio increases with increasing sSFR and decreasing metallicity. For *Ion2* the observed ratio is ≥ 15 making *Ion2* as an outlier in the Oxygen abundance vs. [O III]/[O II] ratio relation and the $\text{EW}(\text{H}\beta)$ (i.e., sSFR) vs. [O III]/[O II] ratio (Figure 2, Stasińska et al. 2015): *Ion2* ratio is higher by ~ 0.6 dex for the observed $\text{EW}(\text{H}\beta)$ and the ratio is higher by ~ 1 dex compared to galaxies in the SDSS sample with similar metallicities. The *Ion2* [O III]/[O II] ratio is also higher than what is expected for the derived stellar mass, SFR, and sSFR (Nakajima & Ouchi 2014). Therefore, we conclude that the extreme [O III]/[O II] ratio is due to unusual physical conditions (density-bounded nebula), which imply a low column density of neutral gas, and so favor leakage of ionizing photons (Nakajima & Ouchi 2014).

4 Conclusions

We present new observations with the Keck/MOSFIRE NIR spectrograph and a new analysis of the UV spectrum of a Lyman continuum emitter candidate. Our main results can be summarized as follows:

- a new analysis of the UV spectrum shows a signal consistent with a direct detection of ionizing photons with $S/N > 5$;

- the Ly α emission at the systemic redshift, the high Ly α escape fraction, the non detection of low-ionization absorption lines are consistent with a low neutral hydrogen column density, while velocity separation of the two Ly α peaks is in tension with expectation (e.g., Verhamme et al. 2015);
- we find low metallicity ($\sim 1/6Z_{\odot}$), strongly subsolar C/O ratio and high ionization parameter ($\log U = -2.25$) using a T_e -consistent method, in good agreement with previous results at $z \sim 2 - 3$;
- *Ion2* exhibit one of the largest [O III]/[O II] ratio observed at $z > 3$ and similar large ratios are predicted for galaxies with low metallicities and Lyman continuum leakage (Nakajima & Ouchi 2014);

A complete analysis of *Ion2* can be found in de Barros et al. (2015). In the near future, our approved proposal to observe *Ion2* with *HST*/F336W will hopefully shed new light on the nature of this source (PI: Vanzella).

We thank M. Tosi, F. Annibali, M. Brusa and H. Atek for useful discussions. We acknowledge the financial contribution from PRIN-INAF 2012.

References

- Amorín, R., Grazian, A., Castellano, M., et al. 2014a, ApJ, 788, L4
 Amorín, R., Pérez-Montero, E., Contini, T., et al. 2015, A&A, 578, A105
 Amorín, R., Sommariva, V., Castellano, M., et al. 2014b, A&A, 568, L8
 Amorín, R. O., Pérez-Montero, E., & Vílchez, J. M. 2010, ApJ, 715, L128
 Borthakur, S., Heckman, T. M., Leitherer, C., & Overzier, R. A. 2014, Science, 346, 216
 Boutsia, K., Grazian, A., Giallongo, E., et al. 2011, ApJ, 736, 41
 Bridge, C. R., Teplitz, H. I., Siana, B., et al. 2010, ApJ, 720, 465
 Bruzual, G. & Charlot, S. 2003, MNRAS, 344, 1000
 Cen, R. & Kimm, T. 2015, ApJ, 801, L25
 de Barros, S., Vanzella, E., Amorín, R., et al. 2015, ArXiv e-prints [arXiv] 1507.06648
 Ferland, G. J., Porter, R. L., van Hoof, P. A. M., et al. 2013, λ , 49, 137
 Grazian, A., Fontana, A., Santini, P., et al. 2015, A&A, 575, A96
 Inoue, A. K. & Iwata, I. 2008, MNRAS, 387, 1681
 Inoue, A. K., Shimizu, I., Iwata, I., & Tanaka, M. 2014, MNRAS, 442, 1805
 Jaskot, A. E. & Oey, M. S. 2014, ApJ, 791, L19
 Ly, C., Malkan, M. A., Nagao, T., et al. 2014, ApJ, 780, 122
 Malkan, M., Webb, W., & Konopacky, Q. 2003, ApJ, 598, 878
 Maseda, M. V., van der Wel, A., Rix, H.-W., et al. 2014, ApJ, 791, 17
 Mostardi, R. E., Shapley, A. E., Nestor, D. B., et al. 2013, ApJ, 779, 65
 Mostardi, R. E., Shapley, A. E., Steidel, C. C., et al. 2015, ApJ, 810, 107
 Nakajima, K. & Ouchi, M. 2014, MNRAS, 442, 900
 Nestor, D. B., Shapley, A. E., Kornei, K. A., Steidel, C. C., & Siana, B. 2013, ApJ, 765, 47
 Pérez-Montero, E. 2014, MNRAS, 441, 2663
 Shapley, A. E., Steidel, C. C., Pettini, M., Adelberger, K. L., & Erb, D. K. 2006, ApJ, 651, 688
 Siana, B., Shapley, A. E., Kulas, K. R., et al. 2015, ApJ, 804, 17
 Siana, B., Teplitz, H. I., Ferguson, H. C., et al. 2010, ApJ, 723, 241
 Stasińska, G., Izotov, Y., Morisset, C., & Guseva, N. 2015, A&A, 576, A83
 Steidel, C. C., Pettini, M., & Adelberger, K. L. 2001, ApJ, 546, 665
 Vanzella, E., de Barros, S., Castellano, M., et al. 2015, A&A, 576, A116
 Vanzella, E., Fontana, A., Pentericci, L., et al. 2014, A&A, 569, A78
 Vanzella, E., Guo, Y., Giavalisco, M., et al. 2012, ApJ, 751, 70
 Vanzella, E., Siana, B., Cristiani, S., & Nonino, M. 2010, MNRAS, 404, 1672
 Verhamme, A., Orlitová, I., Schaerer, D., & Hayes, M. 2015, A&A, 578, A7
 Yang, H., Malhotra, S., Gronke, M., et al. 2015, ArXiv e-prints [arXiv] 1506.02885